Journal of Environmental Management 299 (2021) 113452

Contents lists available at ScienceDirect

Journal of Environmental Management

journal homepage: www.elsevier.com/locate/jenvman

The morphometric acclimation to depth explains the long-term resilience of the seagrass *Cymodocea nodosa* in a shallow tidal lagoon

G. Peralta [a,*], O. Godoy [a], L.G. Egea [a], C.B. de los Santos [a,b], R. Jiménez-Ramos [a], M. Lara [a,c], F. G. Brun [a], I. Hernández [a], I. Olivé [a,d], J.J. Vergara [a], V. González-Ortiz [a], F. Moreno-Marín [a], E. P. Morris [a], B. Villazán [a,e], J.L. Pérez-Lloréns [a]

[a] Department of Biology, University of Cadiz, Spain
[b] Centre of Marine Sciences, University of Algarve, Portugal
[c] Dpto. Ecología y Geología, University of Malaga, Spain
[d] Stazione Zoologica Anton Dohrn, Italy
[e] TAXUS Medio Ambiente S.L., Spain

ARTICLE INFO

Keywords:
Cymodocea nodosa
Seagrasses
Time-series
Biomass
Leaf growth and loss rates
Meadow production

ABSTRACT

Cadiz Bay is a shallow mesotidal lagoon with extensive populations of the seagrass *Cymodocea nodosa* at intertidal and shallow subtidal elevations. This work aims to understand the mechanisms behind the resilience of this species to gradual sea level rise by studying its acclimation capacity to depth along the shallow littoral, and therefore, to gradual variations in the light environment. To address this objective, these populations have been monitored seasonally over a 10 year period, representing the longest seasonal database available in the literature for this species. The monitoring included populations at 0.4, −0.08 and −0.5 m LAT. The results show that *C. nodosa* has a strong seasonality for demographic and shoot dynamic properties – with longer shoots and larger growth in summer (high temperature) than in winter (low temperature), but also some losses. Moreover, shoots have different leaf morphometry depending on depth, with small and dense shoots in the intertidal areas (0.4 m) and sparse large shoots in the subtidal ones (−0.08 and 0.5 m). These differences in morphometry and shoot dynamic properties, combined with the differences in shoot density, explain the lack of differences in meadow production balance (i.e. meadow growth – meadow losses) between the intertidal (0.4 m) and the deepest population (−0.5 m), supporting the long term resilience of *Cymodocea nodosa* in Cadiz Bay. This study contributes to the understanding of the mechanisms behind seagrass stability and resilience, which is particularly important towards predicting the effects of climate change on these key coastal ecosystems, and also highlights the value of continuous long-term monitoring efforts to evaluate seagrass trajectories.

1. Introduction

Seagrass meadows are important coastal habitats with valuable benefits for people and the planet (UNEP, 2020). They play a significant global role in supporting food security (Unsworth et al., 2019) and mitigating climate change through carbon sequestration and storage (Fourqurean et al., 2012; Duarte et al., 2013) and ocean acidification amelioration (Ricart et al., 2021). They also enrich biodiversity through habitat provision (Sievers et al., 2019; Lefcheck et al., 2019), purify water by removing nutrients, sediments and contaminants (de los Santos et al., 2020 Laffrata et al., 2019), protect the coastline (Ondiviela et al., 2014), and control diseases (Lamb et al., 2017). Seagrass meadows are also acknowledged for transferring organic matter and nutrients to adjacent systems (Gillis et al., 2014; Huxham et al., 2018 . Egea et al., 2019a) and for connecting marine fauna with other ecosystems (Dorenbosch et al., 2004; Heck et al., 2008; Unsworth et al., 2008), making them key elements in the functioning and connectivity between ecosystems along the seascape.

As with many other coastal ecosystems, seagrasses are facing growing anthropogenic threats, mostly water quality deterioration and coastal modification, resulting in seagrass loss and degradation (Orth et al., 2006; Waycott et al., 2007; de los Santos et al., 2019; Dunic et al., 2021). The global seagrass decline is expected to have a severe impact on human wellbeing, causing losses of fisheries (Lefcheck et al., 2017),

* Corresponding author.
E-mail address: gloria.peralta@uca.es (G. Peralta).

https://doi.org/10.1016/j.jenvman.2021.113452
Received 31 May 2021; Received in revised form 27 July 2021; Accepted 30 July 2021
Available online 8 September 2021

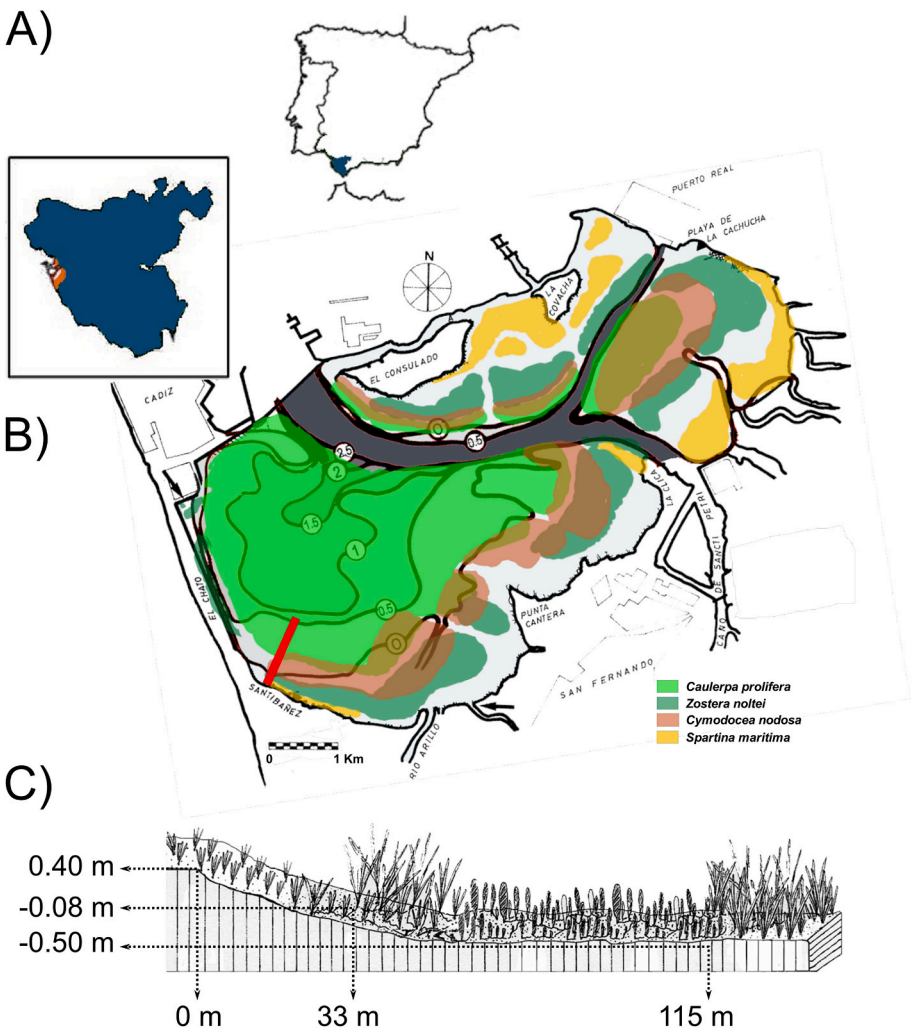

Fig. 1. Cadiz Bay and sampling locations. A) Location of Cadiz Bay in Spain and zoom-in of the province of Cadiz (Cadiz Bay highlighted in orange). B) Detail of the inner body of the bay with the distribution of dominant benthic macrophytes, and the isobaths. Red rectangle on the left bottom side of the image corresponds to the sampled area (Santibañez). (Modified from Muñoz and Sanchez-LaMadrid, 1994). C) Elevation (m LAT) and relative horizontal positions of the sampling sites in the study area. (For interpretation of the references to colour in this figure legend, the reader is referred to the Web version of this article.)

water quality, shoreline stability, and ecosystem richness (Orth et al., 2006). Moreover, climate change is expected to contribute to continued seagrass decline in the temperate zone and poleward expansion in the Northern Hemisphere (Hyndes et al., 2017). Therefore, evaluating the resilience of seagrass meadows and obtaining knowledge about the underlying drivers and processes involving such transition is necessary if adaptation is to be managed.

At a global scale, averages of 0.3–4.8 °C increase in sea surface temperature and 0.26–0.82 m in sea level rise are expected by the end of the 21st century (estimations corresponding to the extremes of the range for RCP2.6 and RCP8.5 respectively; IPCC, 2014). Since these variations are expected to be gradual (IPCC, 2014), understanding the mechanisms ruling seagrass acclimation is going to be crucial in comprehending the key processes behind the long-term resilience of seagrasses on changing environments. This knowledge requires the study of short- and long-term mechanisms under a broad spectrum of environmental changes (Hughes et al., 2018). Unfortunately, long-term studies evaluating the resilience of seagrass species are scarce (Roca et al., 2016).

Besides anthropogenic disturbances, the evaluation of seagrass acclimation under natural conditions requires the existence of environmental gradients wide enough to support measurable differences in seagrass response. Considering light as the most sensitive driver for seagrass success (Hemminga and Duarte, 2000), shallow environments and their associated light gradients offer an excellent framework for understanding key mechanisms behind seagrass acclimation and resilience (understanding here resilience as the "capacity of an ecosystem to absorb disturbances and adapt to change without switching to an alternative stable state"; Holling, 1973).

Cadiz Bay is an Atlantic shallow environment protected from the swell and with high water turnover rate (Alvarez et al., 1997). The pressure of intensive agriculture is low and fish farming mainly extensive (Junta de Andalucía, 2015), making the most threatening pressures those related to physical disturbances of muddy sediments (e.g. shell fishing, boat anchoring and mooring in some areas of the bay; Barragan-Muñoz and Andrés-García, 2020). This type of pressures modifies sediment stability with consequences for vegetation survival (Collins et al., 2010) and, indirectly, for light availability. From low intertidal to shallow subtidal elevations, the benthos of Cadiz Bay is covered by dense populations of *Cymodocea nodosa* (aprox. 800; ha, Morris et al., 2009). In the Gulf of Cadiz, *C. nodosa* is close to its northern Atlantic distribution limit (Short et al., 2010). This implies that in scenarios of climate change, temperature rise is not expected to be crucial for the survival of this species, offering a good opportunity to focus mainly on adaptations to light gradients, and therefore, to sea level rise. *Cymodocea nodosa* is a medium-size, fast-growing seagrass with proven morphometric plasticity and capable of colonizing very different environments (de los Santos et al., 2013; Máñez-Crespo et al., 2020), making this species an excellent model for studying seagrass acclimation to gradual environmental changes.

This work aims to understand the mechanisms behind the resilience of *C. nodosa* by studying the acclimation capacity of this species to depth along the shallow littoral, and accordingly, to gradual variations in the light environment. To meet this objective, we used the longest seasonal database available for this species (10 years). This database includes

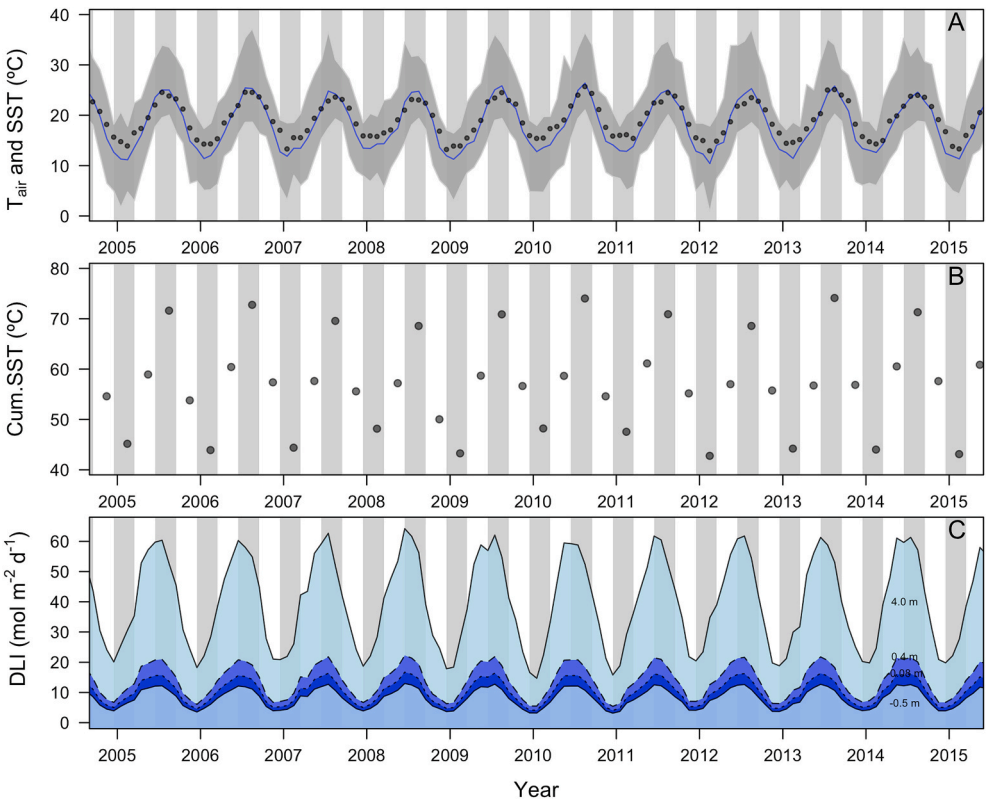

Fig. 2. Environmental variables for Cadiz Bay during the study period (2005–2015). A) Monthly averaged air temperature (T_{air}, °C, blue line), monthly minimum and maximum air temperature (dark grey ribbon), and monthly averaged Sea Surface Temperature (SST, °C, black dots). B) Cumulative SST per season (°C season^{-1}). C) Monthly averages of Daily Light Integration (DLI, mol photons m^{-2} d^{-1}) at surface irradiance (4.0 m), intertidal (0.4 m), edge subtidal (−0.08 m) and subtidal (−0.5 m) elevations. Seasons are indicated as alternated grey and white bands on the background. (For interpretation of the references to colour in this figure legend, the reader is referred to the Web version of this article.)

demographic variables and dynamic morphometric traits of *C. nodosa* plants growing at different depths. This allows characterizing the morphometric acclimation mechanisms that take place over time (seasonal and interannual) and depth responsible for the resilience of the natural populations of *C. nodosa* distributed in the shallow elevations of Cadiz Bay (Spain).

2. Material and methods

2.1. Sampling site

Cadiz Bay is an Atlantic shallow environment located in SW Spain (36° 23' - 36° 37′N and 6° 8' - 6° 15′W, Fig. 1A). It is formed by two water bodies (external and internal bays) well communicated by tides through a narrow strait. Despite the surroundings of the bay being densely populated (5 cities with more than 400,000 inhabitants), the ecological value for local biodiversity and migrating waterfowls (Pérez-Hurtado et al., 1997) is recognized through protection features such as 'Specially Protected Area' (SPA) and 'Special Area of Conservation' (SAC) according to the European legislation (Birds Directive 79/409/CEE, ES0000140 2006/613/CE, Decreto 493/2012, EU Habitats Directive 92/43/CEE, ES6120009 2006/613/CE, Decreto 369/2015), and it is a declared Natural Park (Law 2/1989/CA) and RAMSAR site (1265, 24/10/02).

The sampling area was located in the inner water body of the bay of Cadiz. This is a shallow embayment (mean 3 m LAT, Muñoz and Sanchez-LaMadrid, 1994), protected from the swell under a mesotidal and semidiurnal tidal regime (mean tidal range 2.3 m and mean spring tidal range 3.7 m; del Río et al., 2012). The combination of depth and tidal regime facilitates a high water turnover rate (up to 75% per tidal cycle, Alvarez et al., 1997). The seabed of the inner bay is profusely vegetated (Muñoz and Sanchez-LaMadrid, 1994; Morris et al., 2009) exhibiting a zonation from saltmarsh plants on the high intertidal area (mainly *Sarcocornia* spp. and *Spartina maritima*) to dense populations of the chlorophyte *Caulerpa prolifera* at the subtidal one (Fig. 1B). The intermediate elevations are covered by sequential belts of the seagrasses *Zostera noltei,* in the intertidal, and *C. nodosa,* in the intertidal and shallow subtidal areas (Fig. 1B and C). Scattered patches of *Zostera marina* also thrive within the distribution area of *C. nodosa* (Brun et al., 2015).

Our study was carried out in the *C. nodosa* beds of the Santibáñez area (red rectangle in Fig. 1B) and the sites for sampling were selected according to the elevation including 0.4 (intertidal), −0.08 (edge subtidal) and −0.5 (subtidal) m (Fig. 1C). From here on, all elevations expressed in this work refer to the Lowest Astronomical Tide (LAT).

2.2. Environmental variables

The environmental information for Cadiz Bay was obtained from remote sensing facilities. Data were acquired for latitude 36.542, longitude −6.250 using a 15 min integration period. The meteorological data (air temperature, wind speed, wind direction and rainfall at an altitude of 36 m) were obtained from the MERRA-2 service. The radiation data were obtained at 0 m altitude from Global irradiation on horizontal plane at ground level (GHI, Wh m^{-2}) from the CAMS Radiation Service v2.7 all-sky irradiation (derived from satellite data).

Additionally, the monthly sea surface temperature (SST) was acquired from the Level-3 MODIS-Aqua imagery (Moderate Resolution Imaging Spectroradiometer). Polygons of 5 and 30 km^2 were delimited in the deepest zone of the inner and outer bay, respectively. Monthly averaged temperatures within each polygon were estimated from daily images and a spatial resolution of 500-m. The images were processed in the code editor with JavaScript in Google Earth Engine (https://developers.google.com/earth-engine/datasets/catalog/NASA_OCEANDATA_MODIS-Aqua_L3SMI). Air temperature data were monthly averaged, computing also minimum and maximum values. Additionally, the cumulative SST was calculated as the accumulation of 3 SST values per season. This procedure has proven to increase the capacity to detect effects of temperature on biological variables (Shaltout and Omstedt, 2014). The values of the cumulative SST formed three groups around 48,

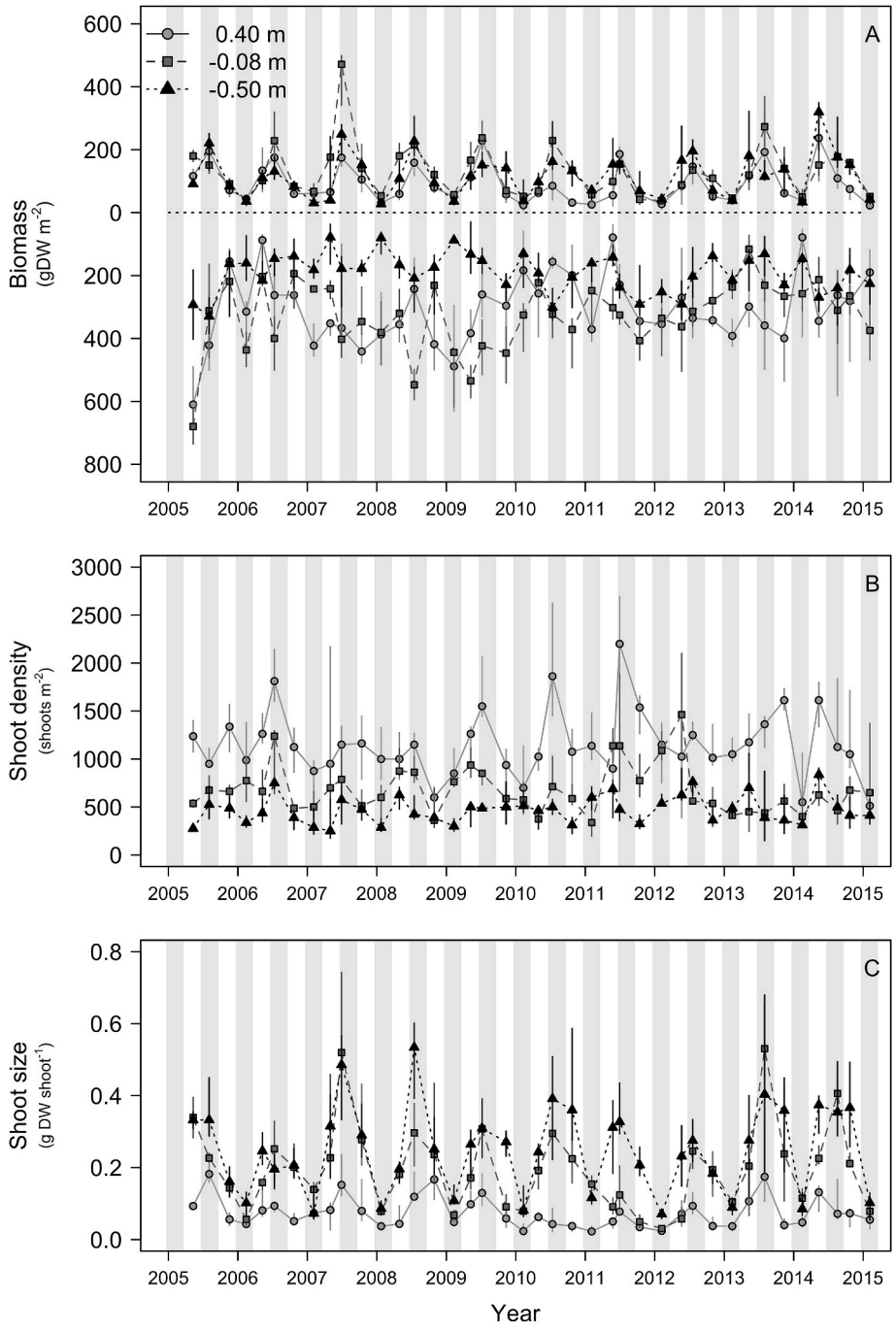

Fig. 3. Temporal changes in *Cymodocea nodosa* demographic variables at Cadiz Bay. A) Leaf (top) and belowground (bottom) biomass, B) Shoot density and C) Shoot size. The variables are evaluated at intertidal (0.4 m), edge subtidal (−0.08 m) and subtidal elevations (−0.5 m). Data points represent medians and error bars represent first and third quantiles.

57 and 69 °C season^{-1}, which correspond to winter, spring and fall, and summer respectively. These values were used to statistically analyze the effect of seasonality (as a categorical variable) on *C. nodosa* variables. Moreover, this method allows comparison of the temporal effect of seasonality versus a potential interannual trend and, finally, whether there are interactions between seasonality, interannual trend, and elevation.

The tidal information was obtained from a time-series (15 min, 2004–2015) of the sea level of the "Cadiz III" tide gauge and the R package 'Tides'. The radiation data are shown as Daily Light Integral values (DLI; mol photons m^{-2} d^{-1}), with values corresponding to surface irradiance (4.0 m) and the studied elevation gradient (0.4, −0.08, and −0.5 m). To estimate these DLI values, the GHI data (Wh m^{-2}) were converted into PAR (Photosynthetically Active Radiation; μmol photons m^{-2} s^{-1}), by using the *sw. to.par.base* function (Winslow et al., 2016), multiplying by 1/0.25 and integrating the irradiance per day (mol photons m^{-2} d^{-1}). The DLI values at the elevations were estimated, taking into account the effects of tides on the sea level and using the Beer-Lambert law according to the model described in Morris et al. (2009), and using a mean attenuation coefficient (K_d) of 0.6 m^{-1} (Olivé et al., 2013). The effects of wind, or any other variable with potential effects on water turbidity, were disregarded.

Table 1
ANOVA for the best linear mixed effects (lme) models for demographic variables of *Cymodocea nodosa*. Demographic variables: AG: Leaf biomass, BG: Belowground biomass, Density: Shoot density, SDW: Shoot size. Fix predictors: Elevation, Temperature (cumulative SST), Year. The values represent "numerator DF (denominator DF) F" and p-values: ns: not significant, *<0.05, **<0.01, ***< 0.001. The structures of the corresponding models are given at the bottom of the table.

Covariates	AG[a]	BG[b]	Density[c]	SDW[d]
Elevation	2 (15)	2 (15)	2 (15)	2 (15)
	28.2***	58.4***	211.1***	195.9***
Temperature	1 (684)	1 (682)	1 (681)	1 (685)
	634.2***	0.02^{ns}	58.8***	336.9***
Year	1 (684)	1 (682)	1 (681)	
	0.00^{ns}	3.5^{ns}	0.8^{ns}	
Elevation*Temperature		2 (682)	2 (681)	2 (685)
		6.07**	3.8*	4.6*
Elevation*Year	2 (684)	2 (682)	2 (681)	
	4.6*	6.03**	5.0*	
Temperature*Year		1 (679)	1 (681)	
		1.19^{ns}	8.6*	
Elevation*Temperature*Year		2 (679)		
		3.22*		
Model weight	0.52	0.53	0.51	0.50

[a] log(AG) ~ Elevation + Temperature + Year + Elevation*Year + 1.
[b] log(BG) ~ Elevation + Temperature + Year + Elevation * Temperature + Elevation * Year + 1.
[c] log(density) ~ Elevation + Temperature + Year + Elevation * Temperature + Elevation * Year + Temperature * Year + Elevation * Temperature * Year + 1.
[d] log(SDW) ~ Elevation + Temperature + Elevation * Temperature + 1.

2.3. Seagrass sampling design

The biological variables of *C. nodosa* were monitored seasonally over a period of 10 years (spring 2005 - winter 2015) at 0.4, −0.08 and −0.5 m. The samplings were performed thanks to the contribution of the monitoring program FAMAR (https://famar.wordpress.com/voluntariado/), coordinated by a scientist of the Department of Biology of the University of Cadiz.

For demographic variables, a total of six random samples (0.04 m^2 per sample) per elevation and season were considered. The samples were carefully collected during low tide around days 30, 45 and 60 of each season, harvesting two samples per day and elevation. The architectural and dynamic attributes of *C. nodosa* were studied using a punching method (Peralta et al., 2000) in 10–15 shoots per elevation and season. For this method, the inner leaf of the shoots is marked and all individual leaves measured (±0.5 cm) *in situ*, and then collected after 26–32 days for laboratory analysis.

2.4. Laboratory plant analysis

The biomass samples were separated into leaves, rhizomes and roots, and oven-dried (60 °C) until reaching a constant dry weight (DW) to obtain the above-ground (AG, leaves) and below-ground (BG, rhizomes and roots) biomass (g DW m^{-2}). Shoot density (shoots m^{-2}) was also estimated before drying. The shoot size (g DW $shoot^{-1}$) was estimated from the relationship between leaf biomass and shoot density.

The analysis of marked shoots included the measurement of the individual leaves in length (leaf length, LL, cm) and weight (g DW) (see Peralta et al., 2000 for further details). The plant dynamic traits estimated from these measurements are leaf appearance rate (LAR, leaves $shoot^{-1}$ d^{-1}, eq. (1)) leaf growth rate (LGR, mg DW $shoot^{-1}$ d^{-1}, eq. (2)), and leaf loss rate (LLR, mg DW $shoot^{-1}$ d^{-1}, eq. (3)).

$$LAR = \frac{\sum NL}{t_f - t_o} \quad (1)$$

$$LGR = \left(\frac{\sum_{i=1}^{n}\left[\left(LL_{i,f} - LL_{i,0}\right) > 0\right]}{t_f - t_0}\right) * \frac{DW}{LL} \quad (2)$$

$$LLR = \left(\frac{\sum_{i=1}^{n}\left[\left(LL_{i,f} - LL_{i,0}\right) < 0\right] - \sum_{i=1}^{m} LL_{i,0}}{t_f - t_0}\right) * \frac{DW}{LL} \quad (3)$$

where: *NL* represents the new leaves that appeared in between the punching (t_0) and collecting day (t_f), *LL* is the leaf length (cm); subscript i refers to the ith leaf within the shoot; *n* is the number of leaves at the end of the studied period; m is the number of leaves lost during the studied period; subscripts f and 0 refer, respectively, to final and initial conditions; t_f - t_0 is the studied period (d); *DW/LL* is the dry weight/length ratio for leaves (g DW cm^{-1} leaf), and NL_a is the number of new leaves generated during the study period.

Finally, the meadow processes estimated from demographic properties and the dynamic traits of the shoots were meadow production (*MP*, g DW m^{-2} $season^{-1}$; eq. (4)), meadow losses (*ML*, g DW m^{-2} $season^{-1}$; eq. (5)), and meadow production balance (*MPB*, g DW m^{-2} $season^{-1}$, eq. (6)).

$$MP = LGR_{q2} * Density_{q2} * t_s \quad (4)$$

$$ML = LLR_{q2} * Density_{q2} * t_s \quad (5)$$

$$MPB = MP - ML \quad (6)$$

where: LGR_{q2}, LLR_{q2} and $Density_{q2}$ are respectively the medians of the LGR, LLR and the shoot density for the corresponding elevation and season, and t_s the number of days of the season.

Unfortunately, in a few cases all marked shoots were lost. In those cases, and for graphical purposes only, the corresponding value was replaced by the corresponding elevation-specific seasonal value obtained from the entire data set (2005–2015). These particular cases are highlighted in the corresponding figures and were not included in the statistical analysis.

2.5. Statistical analysis

We performed generalized linear mixed models (GLMMs) to test the resilience of *C. nodosa* and its underlying morphometric mechanisms. This was done following a two-step approach. First, we compared models using Akaike Information Criteria (AIC) that contained different combinations of temporal random structures. Specifically, we considered different temporal autocorrelation structures following a *CorARMA* (p,q) approach in the package "nlme" (Pinheiro et al., 2019). In this temporal autocorrelation structure p and q represent, respectively, the autoregressive order (t-1, t-2 etc.) and the moving average order of the ARMA structure. Overall we considered two time lag orders for p (1, 2) and three moving average orders for q (1, 2, 3) following this combination of (p,q) (1, 1; 1, 2; 2, 2; 2, 3). We also weighted observations by season (winter, spring, summer and fall) because we observed differences in data dispersion within years that were consistent during the time series (see error bars in Fig. 3 and Fig. 5). Best models (i.e., lowest AIC) were always those that included an ARMA temporal autocorrelation structure (in most cases p = 1), and the weight of season to account for overdispersion.

We then analyzed the fixed part of the models in which elevation (3 levels: 0.4 m or intertidal, −0.08 m or edge subtidal and −0.5 m or subtidal), cumulative SST (3 levels: 48, 57 and 69 °C $season^{-1}$) and their interactions were included as categorial predictors. The variable year was also included as fixed predictor to evaluate a potential temporal trend in the response variable evaluated (i.e. the response variable does not show a stationary trend during the 10 years of observations). Again, AIC was used to select the best supported model. Where significant differences were found, we performed a post-hoc Tukey's test to determine differences among factors' levels. Prior to any analyses, all

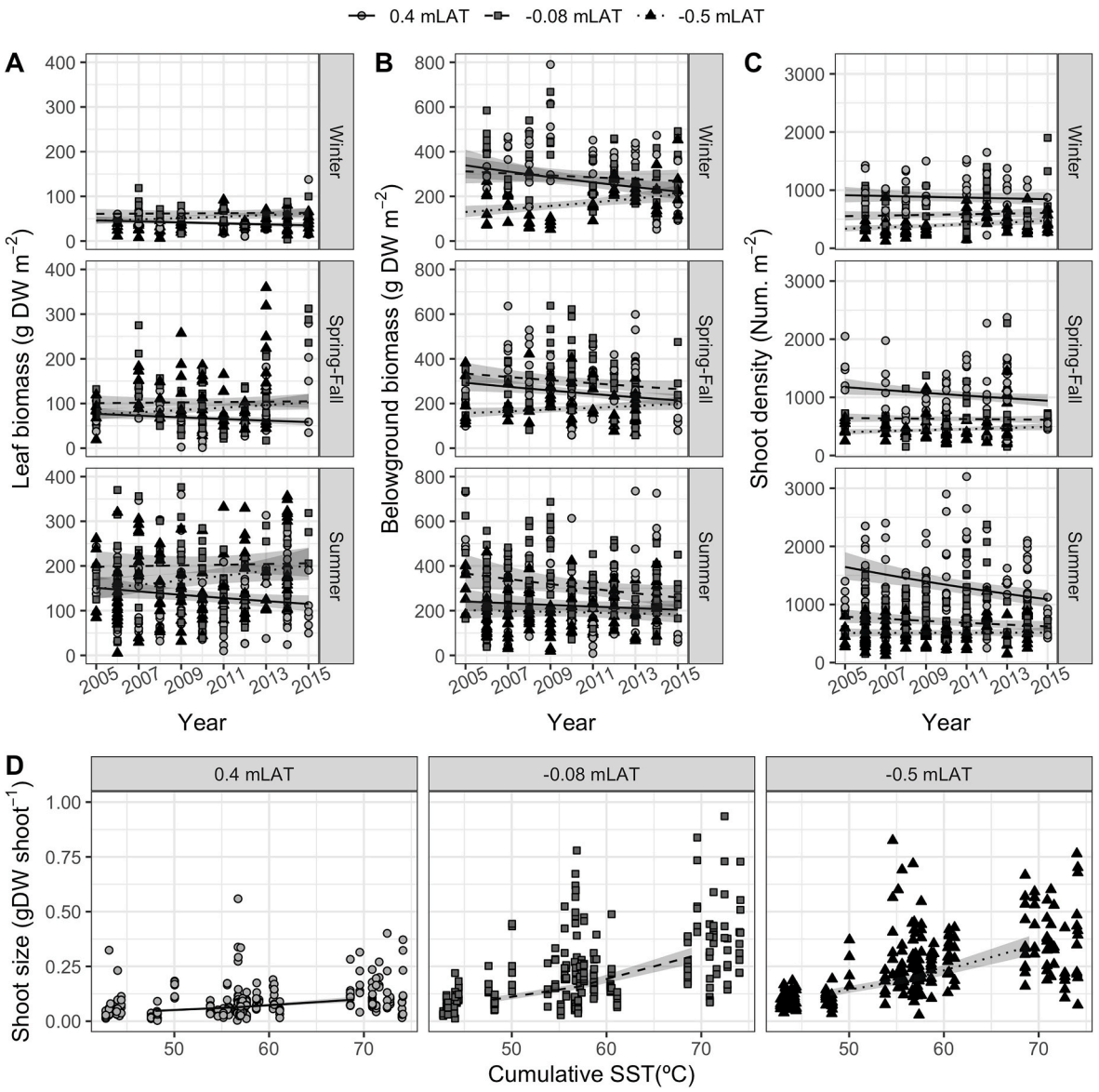

Fig. 4. *Cymodocea nodosa* meadow demography models. Model interpretation for: A) Leaf biomass, B) Belowground biomass, C) Shoot density and D) Shoot size. Models available in Tables 1 and 3. Points represent raw data, lines and grey areas the corresponding models and their SE. Differences in x-axes are due to differences in model predictors (Tables 1 and 3). Cumulative SST is a proxy for seasonality with winter as ca. 48 °C, spring-autumn ca. 57 °C and summer ca. 69 °C, respectively.

variables except meadow growth balance were log-transformed to meet normality and homoscedasticity of the residuals. The parametric assumptions were corroborated in the model residuals through visual inspections (Zuur et al., 2009). All statistical analyses were conducted using the R statistical environment (version 3.5.3; R Core Team, 2019).

3. Results

3.1. Environmental variables

For the studied period (2005–2015), the monthly air temperature in Cadiz Bay was 12.9 ± 1.1 °C (average ± SD) in winter and 24.3 ± 1.2 °C in summer, with maximum peaks of 38 °C (Fig. 2A). The SST was similar, but milder, to air temperature (15.0 ± 1.0 °C in winter and 23.7 ± 0.9 °C in summer; Fig. 2A). In general, the temperature did not show evidence of any particular anomaly during the studied period. When accumulated seasonally, the values of cumulative SST grouped around 48 (in winter), 57 (in spring and fall) and 69 °C (in summer) (Fig. 2B), corresponding to the quartiles 1 to 3. These values were used to account for seasonality within the overall temporal pattern evaluated from 2005 to 2015.

The temporal pattern for incident light was quite regular over the studied period (Fig. 2C, DLI at 4.0 m) with a marked seasonal pattern (55.6 ± 10.0 mol photon m^{-2} d^{-1} in spring-summer and 29.0 ± 11.7 mol photon m^{-2} d^{-1} in fall-winter; mean ± SD). Compared to the incident light at 4.0 m, the availability of light decreased with depth to 65, 74 and 79% at 0.40, −0.08 and −0.5 m, respectively. This translates into an attenuation of 25% (at −0.08 m) and 42% (at −0.5 m) with respect to the intertidal elevation (0.4 m). Since a conservative value for the attenuation coefficient was used (0.6 m^{-1}; Olivé et al., 2013), the simulated differences in light availability among the studied elevations were stable (14, 10 and 8 mol photon m^{-2} d^{-1} as yearly average at 0.4, −0.08 and −0.5 m respectively). However, any process affecting K_d (e.g. strong easterly winds, common in summer) is expected to increase these differences in light availability with depth.

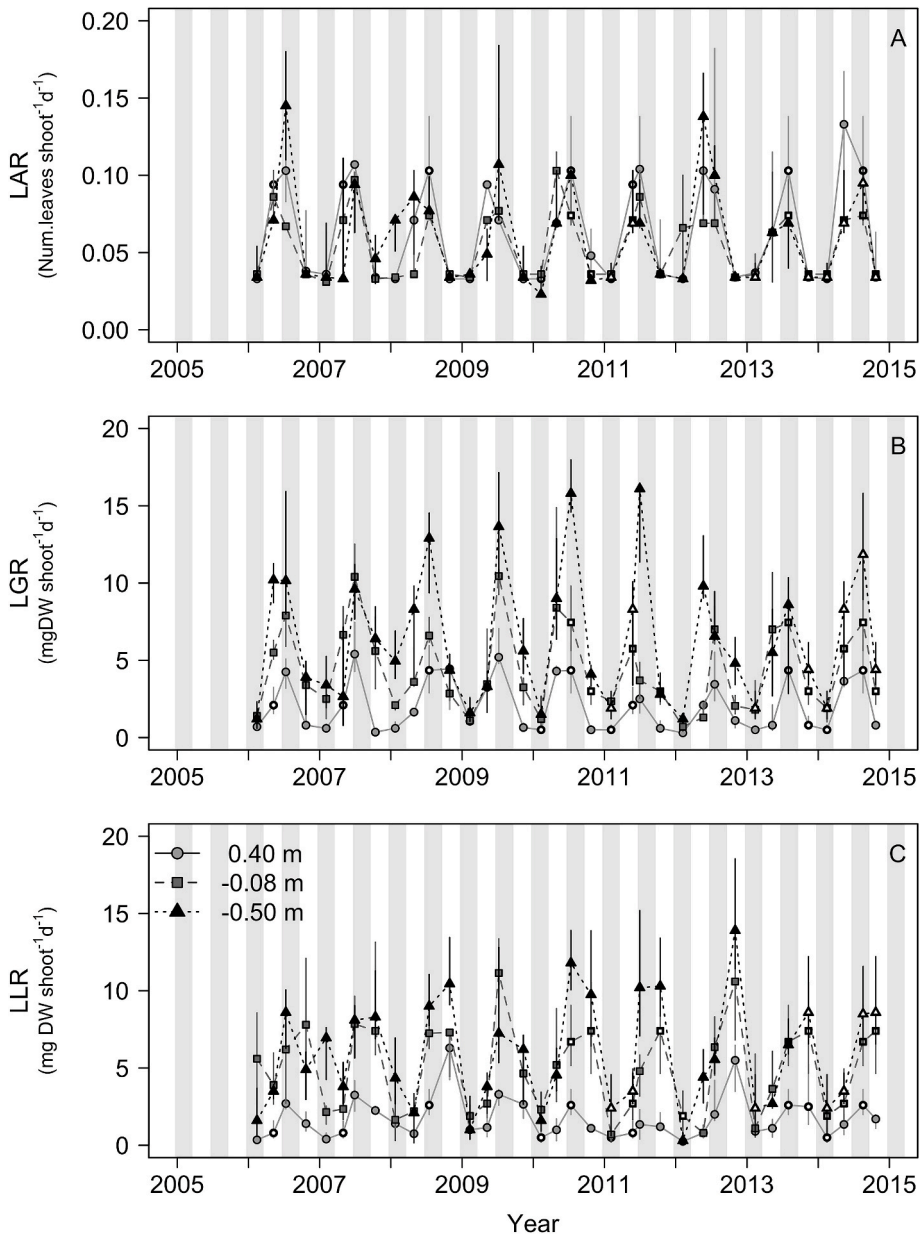

Fig. 5. Temporal changes on *Cymodocea nodosa* shoot processes at Cadiz Bay. A) Leaf appearance rate (LAR), B) Leaf growth rate (LGR) and C) Leaf loss rate (LLR). The variables are evaluated at intertidal (0.4 m), edge subtidal (−0.08 m) and subtidal elevations (−0.5 m). Data points represent medians and error bars first and third quantiles. White core symbols represent missing data replaced by seasonal values. These last values are not included in the statistical analysis.

3.2. Demographic variables

The aboveground biomass of *C. nodosa* showed a marked seasonality with unimodal patterns that were not observed for the belowground biomass (Fig. 3A). The seasonal effect on AG biomass was marked at the three studied elevations, with minimum values in winter (medians 34, 49 and 38 g DW m^{-2} at 0.40, −0.08 and −0.50 m, respectively) and maximum ones in summer (medians 162, 218 and 166 g DW m^{-2} at 0.40, −0.08 and −0.50 m, respectively) (Fig. 3A).

The applied model confirmed that leaf biomass increased with elevation and cumulative SST ('temperature' from here on) (Table 1), having larger biomass in summer and at the subtidal elevations (−0.08 and −0.5 m) than at the intertidal areas (0.4 m) (Fig. 4). Interannual differences were only detected when combined with elevation (Table 1, Fig. 4). In that case, the leaf biomass showed a soft negative trend with year at 0.4 m, a positive one at −0.5 m and a nearly flat trend at the intermediate elevation (−0.08 m) (Fig. 4). The increase in temperature also increased the interannual differences in leaf biomass with depth.

Conversely, belowground biomass did not show a clear seasonal pattern (Fig. 3A bottom series). However, significant differences due to elevation, and its interaction with temperature and year, were detected (Table 1). In general, belowground biomass was similar at 0.4 and −0.08 m, but lower at −0.5 m (medians 298.1, 304.7 and 191.6 g DW m^{-2}, respectively). The interactions of the elevation with temperature and year showed differences among elevations at the beginning of the studied period, but similar values at the end (Fig. 4B). This pattern was attenuated with increasing temperature.

Shoot density also exhibited a seasonal pattern (Fig. 3B) with minimum values in winter (medians 938, 575 and 400 shoots m^{-2} for 0.4, −0.08, −0.5 m, respectively) and maximum ones in summer (1300, 700 and 525 shoots m^{-2} for 0.4, −0.08, −0.5 m, respectively). Both elevation and temperature had significant effects in shoot density (Table 1, Fig. 4C), with higher values at 0.4 m (median 1125 shoots m^{-2}) than at −0.08 m (median 638 shoots m^{-2}), or −0.5 m (median 475 shoots m^{-2}),

Table 2
ANOVA for the best-lme models for plant dynamic variables of *Cymodocea nodosa*. Leaf appearance rate (LAR), Leaf Growth rate (LGR), Leaf loss rate (LLR). Fix predictors: Elevation, Temperature (cumulative SST), Year. The values represent "numerator DF (denominator DF) F″ and p-values: ns: not significant, *<0.05, **<0.01, ***< 0.001. The structures of the corresponding best lme models are at the bottom of the table.

Covariates	LAR[a]	LGR[b]	LLR[c]
Elevation	2 (29) 10.1***	2 (23) 210.5***	2 (23) 90.1***
Temperature	1 (364)	1 (367)	1 (370)
	337.7***	467.7***	156.3***
Year		1 (367) 8.9**	
Elevation*Temperature	2 (364) 4.4*	2 (367) 7.5***	
Model weight	0.37	0.34	0.41

[a] log(LAR) ~ Elevation + Temperature + Elevation * Temperature + 1.
[b] log(LGR) ~ Elevation + Temperature + Year + Elevation * Temperature + 1.
[c] log(LLR + 0.1) ~ Elevation + Temperature + 1.

and a positive effect of temperature that was less evident with increasing depth (Fig. 4C). Multiplicative effects were detected for the paired combinations of year, elevation and temperature (Table 1). These combinations revealed a change in the temporal pattern with depth, going from negative at the intertidal site (0.04 m), to positive at subtidal ones (−0.08 and −0.5 m). This temporal pattern was less evident with increasing temperature, but temperature increased the differences in shoot density between elevations (Fig. 4C).

The seasonal pattern was also clear for shoot size (Fig. 3D), with larger shoots in summer (medians 0.107, 0.354, 0.339 g DW shoot^{-1} in 0.4, −0.08 and −0.5 m respectively) than in winter (medians 0.037, 0.084, 0.089 g DW shoot^{-1} in 0.4, −0.08 and −0.5 m respectively). Elevation, temperature, and their combination had significant effects on shoot size (Table 1, Fig. 4). Temperature had a positive effect on shoot size, significantly larger in subtidal zones (−0.08 y −0.5 m), increasing differences by elevation with increasing temperature (Fig. 4D).

3.3. Plant dynamic variables

Dynamic properties of the shoots showed also a marked seasonality (Fig. 5). Leaf appearance rate (LAR) showed unimodal patterns, with peaks in summer (0.9, 0.8 and 0.9 leaves shoot^{-1} d^{-1} at 0.4, −0.08 and −0.5 m respectively) and minimum values in fall-winter (0.04 leaves shoot^{-1} d^{-1} at 0.4, −0.08 and −0.5 m). Elevation, temperature, and a residual effect of their combination had effects on LAR (Table 2, Fig. 6). Although significant, differences due to elevation where not apparent on visual inspection (Fig. 6).

Leaf growth rate (LGR) showed unimodal patterns, with peaks in summer (4.4, 7.5 and 11.7 mg DW shoot^{-1} d^{-1} at 0.4, −0.08 and −0.5 m respectively) and with minimum values in winter (0.5, 2.1 and 2.1 mg DW shoot^{-1} d^{-1} at 0.4, −0.08 and −0.5 m, respectively). Elevation, temperature and year all had effects on LGR (Table 2, Fig. 6). This variable showed a smooth negative interannual trend and values increased significantly with depth and temperature (Fig. 6).

Leaf loss rate had a similar pattern to that described for growth, with peaks in summer (Figs. 5, 2.6, 6.7 and 8.5 mg DW shoot^{-1} d^{-1} at 0.4, −0.08 and −0.5 m respectively) and valleys in winter (0.5, 1.8 and 2.15 mg DW shoot^{-1} d^{-1} at 0.4, −0.08 and −0.5 m respectively). However, the best fit model only includes elevation and temperature as controlling variable (Table 2), the values of the leaf loss rate showing a significant increase with depth and temperature (Fig. 6).

3.4. Meadow processes

To estimate production and loss at the meadow level, values of growth rate estimated at the level of shoots were scaled up using the corresponding value of shoot density and duration of the season. The results showed how the differences with depth observed at shoot level were partially compensated by differences in shoot density (Fig. 7), but differences were still significant (Table 3), with higher values in production and losses in the subtidal (−0.5 m) than in the intertidal elevation (Fig. 8). Surprisingly, meadow production was lower in the intertidal elevation (median value 140 g DW m^{-2} season^{-1} 0.4 m; Fig. 7A), than in subtidal ones (medians of 230 and 206 g DW m^{-2} season^{-1}, at −0.08 and −0.5 m, respectively).

The differences in meadow production and losses at the extremes of the studied elevation range counterbalanced, resulting in similar values of meadow production balance at 0.4 and −0.5 m (Fig. 8C). In general, the meadow growing at −0.08 m showed lower values in the meadow production balance than in the other two elevations (Fig. 8C). The meadow production balance provides an estimate of net production at the population level. In general, seasonal values of MPB oscillated around zero with negative values in fall and winter and positive ones in spring and summer, which ranged between −400 and 400 g DW m^{-2} season^{-1} (Fig. 7C). Clearly, temperature increased MPB at 0.4 and −0.5 m, but this increase was mild at −0.08 m (Fig. 8C), where the balance had a larger proportion of negative values.

4. Discussion

This study provides the longest seasonal monitoring database for the seagrass *C. nodosa* available in the literature. The observed patterns in morphometric and dynamic variables of the plants lend support to phenotypic plasticity as a principal mechanism for the acclimation of this species. This plasticity is scaled up from shoot to meadow levels, resulting in a balance between gains and losses throughout the seasons. The plasticity of *C. nodosa* enables its acclimation to environmental gradients associated with depth (i.e. light reduction) and seasonality (i.e. light and temperature), highlighting morphometric acclimation as a key strategy for the long-term resilience of *C. nodosa* in shallow environments.

Morphometric acclimation of *C. nodosa* to increasing depth includes maximizing shoot size and decreasing density. These responses to depth, and hence to light availability, have been previously reported for other seagrasses (Pérez-Lloréns and Niell, 1993; Olesen et al., 2017; Enriquez et al., 2019), attributing main benefits for long and sparse plants at deeper locations to better access to light (Krause-Jensen et al., 2000; Collier et al., 2007; Olesen et al., 2017) and for short and dense plants at intertidal and shallower sites to increased resistance to water emersion (Pérez-Lloréns and Niell, 1993; Peralta et al., 2000; Tanaka and Nakaoka, 2004) and as a mechanism for photoprotection (Schubert et al., 2015).

In Cadiz Bay, the leaf traits of *C. nodosa* showed a marked seasonality, with maximum values in summer and minimum in winter for demographic (biomass, shoot density and shoot size, Fig. 3) and dynamic attributes (leaf growth rate, leaf loss rate, Fig. 5). The consistency of this pattern with depth suggests an increase in meristematic activity associated with seasonal increases in light and temperature (Fig. 2; Terrados-Muñoz, 1995; Hemminga and Duarte, 2000). At intertidal elevation, where shoot density is highest, the leaf growth rate could be approaching a growth saturation threshold (Peralta et al., 2002) or a self-thinning limit (Westoby and Howell, 1986; Krause-Jensen et al., 2000; Enriquez et al., 2019). In both cases, the response supports a larger investment in belowground tissues.

The acclimation to depth not only includes differences in shoot size, but also in recruitment (Enriquez et al., 2019). In principle, shoot recruitment is supported by rhizome branching (Hemminga and Duarte, 2000; Brun et al., 2006a), suggesting that adequate environmental conditions for the development of belowground structures could trigger shoot recruitment (Peralta et al., 2002). For *Zostera noltei,* the mechanisms behind shoot size change were previously attributed to combined differences in leaf growth rate and plastochrone index (Peralta et al., 2005; Brun et al., 2007). However, for *C. nodosa*, our results suggest that

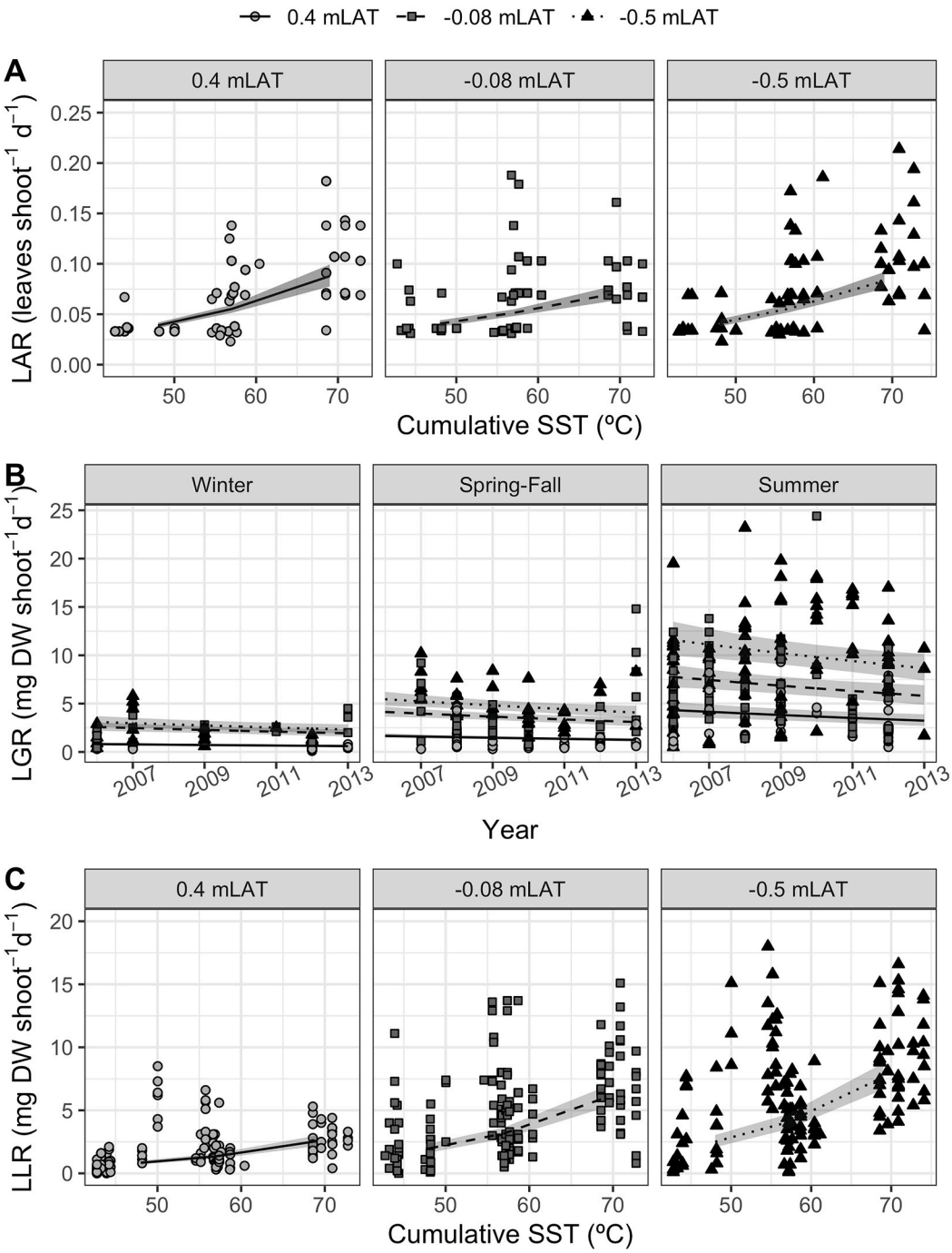

Fig. 6. *Cymodocea nodosa* at shoot level. Model interpretation for shoot dynamic variables: A) Leaf appearance rate (LAR), B) Leaf growth rate (LGR) and C) Leaf loss rate (LLR). Models available in Tables 2 and 3. Points represent raw data, lines and grey areas the corresponding models and their SE. Differences in x-axes are due to differences in model predictors (Tables 2 and 3). Cumulative SST is a proxy for seasonality with winter as ca. 48 °C, spring-autumn ca. 57 °C and summer ca. 69 °C, respectively.

bathymetric differences in shoot size could be related to a lower recruitment of shoots, which can be supported by a lower investment in belowground tissues, and the corresponding larger investment in individual leaves.

In any case, the morphometric acclimation of *C. nodosa* at shoot level (i.e. changes in shoot size and density) clearly rules the dynamic of the meadow. As previously described by Enriquez et al. (2019) for the tropical seagrass *Thalassia testudinum*, our results suggest that the morphometric acclimation of *C. nodosa* compensates at the population level, buffering the consequences of light limitation with depth for meadow production balance and supporting similar aboveground biomass stands along the shallow depth gradient. The observed morphometric response provides a better access to external resources (light and nutrients) with depth, but it also has physiological consequences. Olivé et al. (2013) demonstrated for the same populations of *C. nodosa*, that the subtidal morphotype have larger photosynthetic surface, less self-shading and less tissue respiration than the small intertidal morphotype, helping to compensate for lower light availability and explaining how shoot density decreases with depth faster than biomass (Krause-Jensen et al., 2000).

The morphometric acclimation of *C. nodosa* to depth also includes changes in belowground tissues. Plants growing at the intertidal

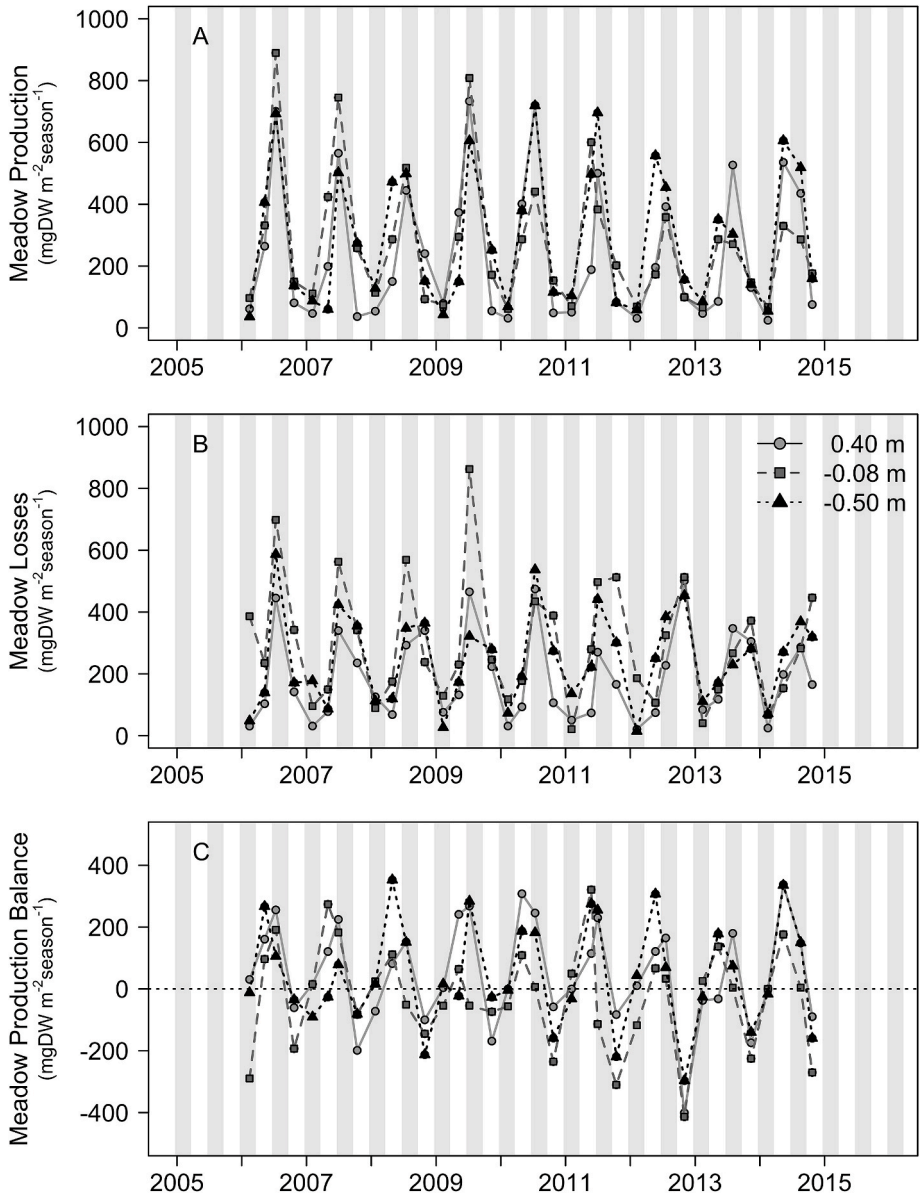

Fig. 7. Seasonality on *Cymodocea nodosa* meadow rates at intertidal (0.4 m), edge subtidal (−0.08 m) and subtidal elevations (−0.5 m) in Cadiz Bay. A) Meadow Production (MP), B) Meadow Losses (ML), C) Meadow Production Balance (MPB).

Table 3
ANOVA for the best-lme models for meadow properties of *Cymodocea nodosa*. Meadow Production (MP), Meadow loss (ML), Meadow Production Balance (MPB). Fix predictors: Elevation, Temperature (cumulative SST), Year. The values represent "numerator DF (denominator DF) F″ and p-values: ns: not significant, *<0.05, **<0.01, ***< 0.001. The structures of the corresponding best lme models are at the bottom of the table.

Covariates	MP[a]	ML[b]	MPB[c]
Elevation	2 (98) 9.6***	2 (101) 13.1***	2 (99) 7.5***
Temperature	1 (98) 14.7***	1 (101) 6.0*	1 (99) 3.05^{ns}
Year	1 (98) 7.1**		
Elevation*Temperature	2 (98) 4.5*		2 (99) 2.6^{ns}
Model weight	0.46	0.39	0.33

[a] log(MP) ~ Elevation + Temperature + Year + Elevation * Temperature + 1.
[b] log(ML) ~ Elevation + Temperature + 1.
[c] MPB ~ Elevation + Temperature + Elevation * Temperature + 1.

elevation exhibited a larger belowground network than the subtidal ones. This is a response previously reported for several seagrass species (Krause-Jensen et al., 2000; Collier et al., 2007; Olesen et al., 2017), being associated with strategies that maintain the carbon balance for the entire plant (Hemminga, 1998). For *Zostera noltei*, it has been stated that production of belowground tissues occurs when the requirements for leaf growth are fulfilled (Peralta et al., 2002), suggesting that the differences on belowground biomass would not necessarily imply light limitation for leaf growth, but optimal light conditions to invest in belowground tissues. This mechanism would favor the spreading of the population by horizontal space occupation and shoot recruitment under higher light availability (with an upper limit defined by the emersion stress, Suykerbuyk et al., 2018), as these conditions favor both production of belowground tissues and shoot recruitment (Duarte and Sand-Jensen, 1990).

Leaf production includes both elongation and generation of new leaves. Once a new leaf is generated, the time for elongation is limited, only the newest 2–3 leaves of every meristem being considered with active growth (Pedersen and Borum, 1993; Brun et al., 2006b).

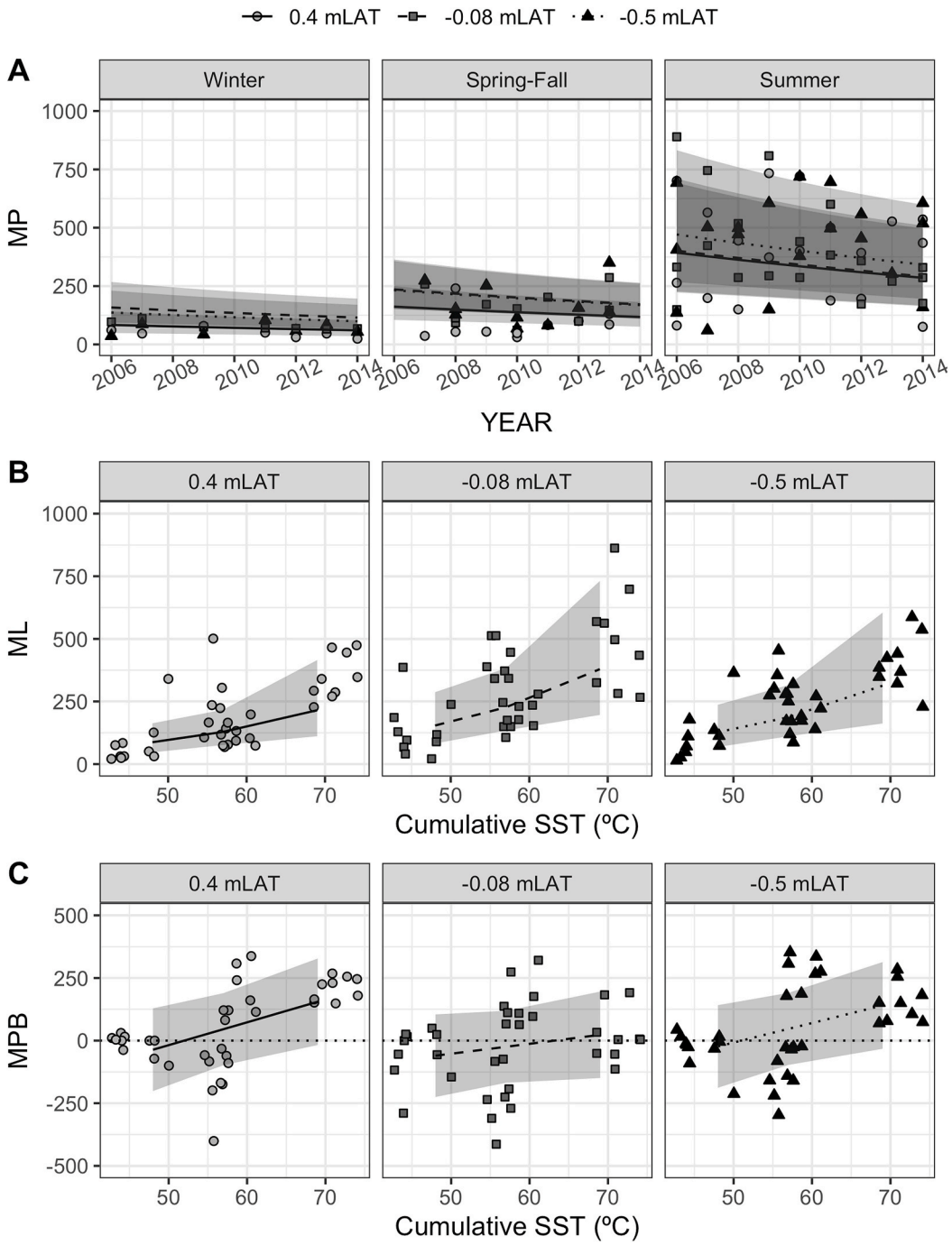

Fig. 8. *Cymodocea nodosa* meadow level models. Model interpretation for seasonal rates of: A) MP: Meadow Production, B) ML: Meadow losses and C) MPB: Meadow Production Balance. Data are expressed in g DW m^{-2} $season^{-1}$. Models available in Table 3. Points represent raw data, lines and grey areas the corresponding models and their SE. Differences in x-axes are due to differences in model predictors (Table 3). Cumulative SST is a proxy for seasonality with winter as ca. 48 °C, spring-autumn ca. 57 °C and summer ca. 69 °C, respectively.

Cymodocea nodosa occurring at Cadiz Bay had a similar rate of leaf appearance (LAR) along depth levels (median ca. 0.09 leaves $shoot^{-1}$ d^{-1} in summer and ca. 0.03 leaves $shoot^{-1}$ d^{-1} in fall-winter, Fig. 5A) and these values are similar to those previously described for this species (Brun et al., 2006a; Sghaier et al., 2017). A similar LAR with depth agrees with the patterns in leaf growth rate (LGR) and leaf loss rate (LLR), as both are larger at subtidal than at intertidal zones, corresponding to the production, or loss, of larger leaves. Summer peaks in growth and losses has been previously described for *C. nodosa* in other locations (Peduzzi and Vukovic, 1990; Cunha and Duarte, 2007). In the case of Cadiz Bay, these peaks were slightly desynchronized, with the peak of LGR starting earlier (spring-summer) and being narrower than the peak of LLR (summer-fall) (Fig. 5). This pattern agrees with the one observed for shoot recruitment and mortality in several temperate seagrass species (Hemminga and Duarte, 2000).

Integrating LGR and LLR (per shoot) with shoot density allows for a preliminary upscaling of morphometric acclimation to population level (meadow production, meadow losses and meadow production balance). These results indicate that the subtidal population has a larger meadow production than the intertidal one, suggesting that light would not limit leaf production at the subtidal zone, or alternatively, that leaf production is also limited at the upper distribution limit (e.g. by emersion or

photoinhibition stresses; Peralta et al., 2002). Similar to meadow production, meadow losses seem to be also lesser at the intertidal elevation. This pattern could be attributed to differences in the size of the senescent leaves, assuming that the senescence rate does not vary with depth, following the observed LAR pattern. What seems clear is that depth differences in growth and losses at shoot level are compensated at population level, resulting in a similar meadow production balance at the extremes of the distribution range (Fig. 7). Only the population occurring at mid elevation (−0,4 LAT) showed a lower meadow production balance. At this elevation, the shoots are large, but so is the belowground biomass, which could act as a burden when faced with periods of low light availability (Hemminga, 1998).

Our results indicate that *C. nodosa* populations at Cadiz Bay have been stable and resilient for (at least) 10 years thanks to a morphometric acclimation strategy. However, it is not clear if this strategy would support the resilience of the seagrass under future climate change scenarios. These scenarios predict sea level rise and temperature increases (IPCC, 2014). According to our results, under these scenarios it could be reasonable to expect a decrease in the meadow production balance as a consequence of the light reduction associated with sea level rise. However, this species has proven to have morphometric acclimation mechanisms that could buffer the consequences of these effects. Previous research has stated that small increases in temperature have positive effects on LGR and carbon community metabolism for the large-leaved subtidal morphotype of *C. nodosa* (Egea et al., 2019a, 2019b), suggesting that negative effects of future scenarios on LGR could be partially offset by an increase in shoot size. On the one hand, the short-leaved morphotype (associated with intertidal elevations) is characterized by a lower AG:BG biomass than the large-leaved morphotype (Fig. 3A). Belowground tissues store reserves that can be important to support clonal expansion towards higher elevations, which is an efficient mechanism to compensate sea level rise effects when the space for accommodation is available. The morphometric acclimation from a short-leaved to a large-leaved morphotype (which could be expected gradually with SLR at the 0.4 m), may increase the resilience of the present population occurring at the intertidal zone.

Our results suggest that a critical element on the resilience of *C. nodosa* in Cadiz Bay is water quality management, since light availability seems to be the main variable forcing *C. nodosa* meadow production balance at Cadiz Bay (Table 3). The water quality degradation in European coastal waters has been one of the major causes of seagrass decline since the 1950s, yet this has been reversed in some locations probably due to the management actions taken to reduce the input of nutrients in coastal waters (de los Santos et al., 2019). The resilience of *C. nodosa* could improve with strategies to regulate activities directly modifying sediment stability and water transparency (e.g. shell fishing or boat anchoring and mooring; Collins et al., 2010), or by regulating activities indirectly affecting water transparency as nutrient loading (i.e. eutrophication; Paar et al., 2021). Lastly, the acclimation strategy of *C. nodosa* also suggest that conservation or restoration of suitable areas to promote population establishment after dispersal is also a complementary strategy to improve the resilience of seagrass meadows.

In summary, *C. nodosa* populations occurring at Cadiz ay in the intertidal-subtidal zone between 0.4 and −0.5 m have been stable during (at least) the last 10 years. Most demographic and dynamic variables evidenced unimodal seasonal patterns with maximum values in summer and minimum ones in winter. Leaf biomass did not differ between the extremes of the studied bathymetric gradient despite the decrease in light availability. This response seems to be due to the morphometric acclimation of the leaves that generated larger, but sparser, shoots with depth. The large-leaved morphotype is more efficient using the available light than the short-leaved one, but also has larger leaf loss rates. At meadow level, the morphometric acclimation, with differences in shoot size and density, support larger leaf production and losses at the subtidal than at the intertidal edge. However, in both cases, they compensate each other in a similar way, supporting similar leaf biomass. Although currently stable, the long-term resilience of this species under climate change scenarios might depend especially on the response of the existing intertidal population. The intertidal population, with a larger belowground investment, could support a gradual horizontal expansion to higher elevations, whereas a gradual morphotype change to larger shoots could improve the use of light availability on the current elevation when sea level rises. The success of these long-term resilience strategies will also depend on the efficiency of the long-term management of water quality and sediment stability of the bay. This study contributes to the understanding of the mechanisms behind seagrass stability and resilience, which is particularly important to predict the effects of climate change on these key coastal ecosystems, and also highlights the value of continuous long-term monitoring efforts to evaluate seagrass trajectories.

The data sets for this article are open access in the Zenodo repository: https://doi.org/10.5281/zenodo.5354868.

Declaration of competing interest

The authors declare that they have no known competing financial interests or personal relationships that could have appeared to influence the work reported in this paper.

Acknowledgements

This work was supported by the Spanish research projects CTM2005-00395/MAR (EVAMARIA), CTM2008-00012 (IMACHYDRO), CTM2011-24482 (SEALIVE) and CTM2017-85365-R (PAVAROTTI). OG acknowledges financial support provided by the Spanish Ministry of Economy and Competitiveness (MINECO) and by the European Social Fund through the Ramón y Cajal Program (RYC-2017- 23666). CBdlS acknowledges support provided by FCT-Foundation for Science and Technology (2020.03825.CEECIND and UIDB/04326/2020).

References

Alvarez, O., Tejedor, B., Tejedor, L., 1997. Simulación hidrodinámica en el área de la Bahía de Cádiz. Análisis de las constituyentes principales. In: IV Jornadas Españolas de Ingeniería de Puertos y Costas, vol. 98. Servicio de Publicaciones de la Universidad Politecnica de Valencia, pp. 125–136.

Barragan-Muñoz, J.M., Andrés-García, M., 2020. The management of the socio-ecological systems of the Bay of Cadiz: new public policies with old instruments? Boletín de la Asociación de Geógrafos Españoles 85 (2866), 1–42. https://doi.org/10.21138/bage.2866.

Brun, F.G., Vergara, J.J., Pérez-Lloréns, J.L., Ramírez, C., Morris, E.P., Peralta, G., Hernández, I., 2015. Diversidad de angiospermas marinas en la bahía de Cádiz: redescubriendo a *Zostera marina*. Chronica naturae 5, 45–56.

Brun, F.G., Cummaudo, F., Olivé, I., Vergara, J.J., Pérez-Lloréns, J.L., 2007. Clonal extent, apical dominance and networking features in the phalanx angiosperm *Zostera noltii* Hornem. Mar. Biol. 151 (5), 1917–1927. https://doi.org/10.1007/s00227-007-0627-y.

Brun, F.G., Vergara, J.J., Peralta, G., García-Sánchez, M.P., Hernández, I., Pérez-Lloréns, J.L., 2006a. Clonal building, simple growth rules and phylloclimate as key steps to develop functional–structural seagrass models. Mar. Ecol. Prog. Ser. 323, 133–148. https://doi.org/10.3354/meps323133.

Brun, F.G., Pérez-Pastor, A., Hernández, I., Vergara, J.J., Pérez-Lloréns, J.L., 2006b. Shoot organization in the seagrass *Zostera noltii*: implications for space occupation and plant architecture. Helgol. Mar. Res. 60, 59–69. https://doi.org/10.1007/s10152-005-0017-0.

Collier, C.J., Lavery, P.S., Masini, R.J., Ralph, P.J., 2007. Morphological, growth and meadow characteristics of the seagrass *Posidonia sinuosa* along a depth-related gradient of light availability. Mar. Ecol. Prog. Ser. 337, 103–115. https://doi.org/10.3354/meps337103.

Collins, K.J., Suonpää, A.M., Mallinson, J.J., 2010. The impacts of anchoring and mooring in seagrass, Studland Bay, Dorset, UK. Underw. Technol. 29 (3), 117–123. https://doi.org/10.3723/ut.29.117.

Cunha, A.H., Duarte, C.M., 2007. Biomass and leaf dynamics of *Cymodocea nodosa* in the ria formosa lagoon, south Portugal. Bot. Mar. 50, 1–7. https://doi.org/10.1515/BOT.2007.001.

de los Santos, C.B., Brun, F.G., Vergara, J.J., Pérez-Lloréns, J.L., 2013. New aspect in seagrass acclimation: leaf mechanical properties vary spatially and seasonally in the temperate species *Cymodocea nodosa* Ucria (Ascherson). Mar. Biol. 160, 1083–1093 s00227-012-2159-3.

de los Santos, C.B., Krause-Jensen, D., Alcoverro, T., Marbà, N., Duarte, C.M., van Katwijk, M.M., Santos, R., 2019. Recent trend reversal for declining European

seagrass meadows. Nat. Commun. 10, 3356. https://doi.org/10.1038/s41467-019-11340-4.
de los Santos, C.B., Olivé, I., Moreira, M., Silva, A., Freitas, C., Araújo Luna, R., Santos, R., 2020. Seagrass meadows improve inflowing water quality in aquaculture ponds. Aquaculture 528, 735502. https://doi.org/10.1016/j.aquaculture.2020.735502.
del Río, L., Plomaritis, T.A., Benavente, J., Valladares, M., Ribera, P., 2012. Establishing storm thresholds for the Spanish Gulf of Cadiz coast. Geomorphology 143–144, 13–23 j.geomorph.2011.04.048.
Dorenbosch, M., van Riel, M.C., Nagelkerken, I., van der Velde, G., 2004. The relationship of reef fish densities to the proximity of mangrove and seagrass nurseries. Estuar. Coast Shelf Sci. 60, 37–48. https://doi.org/10.1016/j.ecss.2003.11.018.
Duarte, C.M., Sand-Jensen, K., 1990. Seagrass colonization: biomass development and shoot demography in *Cymodocea nodosa* patches. Mar. Ecol. Prog. Ser. 67 (1), 97–103. https://doi.org/10.3354/meps067097.
Duarte, C.M., Losada, I.J., Hendriks, I.E., Mazarrasa, I., Marbà, N., 2013. The role of coastal plant communities for climate change mitigation and adaptation. Nat. Clim. Change 3, 961–968. https://doi.org/10.1038/nclimate1970.
Dunic, J.C., Brown, C.J., Connolly, R.M., Turschwell, M.P., Côté, I.M., 2021. Long-term declines and recovery of meadow area across the world's seagrass bioregions. Glob Chang Biol, gcb. 15684. https://doi.org/10.1111/gcb.15684.
Egea, L.G., Barrón, C., Jiménez–Ramos, R., Hernández, I., Vergara, J.J., Pérez–Lloréns, J. L., Brun, F.G., 2019a. Coupling carbon metabolism and dissolved organic carbon fluxes in benthic and pelagic coastal communities. Estuar. Coast Shelf Sci. 227, 106336. https://doi.org/10.1016/j.ecss.2019.106336.
Egea, L.G., Jiménez–Ramos, R., Hernández, I., Brun, F.G., 2019b. Effect of *in Situ* short–term temperature increases on carbon metabolism and dissolved organic carbon (DOC) fluxes in a community dominated by the seagrass *Cymodocea nodosa*. PloS One 14 (1), e0210386. https://doi.org/10.1371/journal.pone.0210386.
Enríquez, S., Olivé, I., Cayabyab, N., Hedley, J.B., 2019. Structural complexity governs seagrass acclimatization to depth with relevant consequences for meadow production, macrophyte diversity and habitat carbon storage capacity. Sci. Rep. 9, 14657. https://doi.org/10.1038/s41598-019-51248-z.
Fourqurean, J.W., Duarte, C.M., Kennedy, H., Marbà, N., Holmer, M., Mateo, M.A., et al., 2012. Seagrass ecosystems as a globally significant carbon stock. Nat. Geosci. 5 (7), 505–509.
Gillis, L.G., Bouma, T.J., Jones, C.G., Van Katwijk, M.M., Nagelkerken, I., Jeuken, C.J.L., et al., 2014. Potential for landscape-scale positive interactions among tropical marine ecosystems. Mar. Ecol. Prog. Ser. 503, 289–303.
Heck, K.L., Carruthers, T.J., Duarte, C.M., Hughes, A.R., Kendrick, G.A., Orth, R.J., Williams, S.L., 2008. Trophic transfers from seagrass meadows subsidize diverse marine and terrestrial consumers. Ecosystems 11, 1198–1210. https://doi.org/10.1007/s10021-008-9155-y.
Hemminga, M.A., 1998. The root/rhizome system of seagrasses: an asset and a burden. J. Sea Res. 39, 183–196. https://doi.org/10.1016/S1385-1101(98)00004-5.
Hemminga, M.A., Duarte, C.M., 2000. Seagrass Ecology. Cambridge University Press.
Holling, C.S., 1973. Resilience and stability of ecological systems. Annu. Rev. Ecol. Systemat. 4, 1–23. https://doi.org/10.1146/annurev.es.04.110173.000245.
Hughes, B.B., Lummis, S.C., Anderson, S.C., Kroeker, K.J., 2018. Unexpected resilience of a seagrass system exposed to global stressors. Global Change Biol. 24, 224–234. https://doi.org/10.1111/gcb.13854.
Huxham, M., Whitlock, D., Githaiga, M., Dencer-Brown, A., 2018. Carbon in the coastal seascape: how interactions between mangrove forests, seagrass meadows and tidal marshes influence carbon storage. Curr Forestry Rep 4, 101–110. https://doi.org/10.1007/s40725-018-0077-4.
Hyndes, G.A., Heck, K.L., Vergés, A., Harvey, E.S., Kendrick, G.A., Lavery, P.S., et al., 2017. Accelerating tropicalization and the transformation of temperate seagrass meadows. Bioscience 66, 938–948. https://doi.org/10.1093/biosci/biw111.
IPCC, 2014. In: Pachauri, R.K., Meyer, L.A. (Eds.), Climate Change 2014: Synthesis Report. Contribution of Working Groups I, II and III to the Fifth Assessment Report of the Intergovernmental Panel on Climate Change [Core Writing Team. IPCC, Geneva, Switzerland, p. 151.
Junta de Andalucía, 2015. Plan Hidrológico del Guadalete-Barbate 2015-2021. Recovered from. http://www.juntadeandalucia.es/medioambiente/portal_web/web/temas_ambientales/agua/planes_hidrologicos/plan_hidrologico2015_2021_gb/memoria_gb.pdf.
Krause-Jensen, D., Middelboe, A.L., Sand-Jensen, K., Christensen, P.B., 2000. Eelgrass, *Zostera marina*, growth along depth gradients: upper boundaries of the variation as a powerful predictive tool. Oikos 91, 233–244. https://doi.org/10.1034/j.1600-0706.2001.910204.x.
Lafratta, A., Serrano, O., Masque, P., Mateo, M.A., Fernandes, M., Gaylard, S., Lavery, P. S., 2019. Seagrass soil archives reveal centennial-scale metal smelter contamination while acting as natural filters. STOTEN 649, 1381–1392. https://doi.org/10.1016/j.scitotenv.2018.08.400.
Lamb, J.B., van de Water, J.A.J.M., Bourne, D.G., Altier, C., Hein, M.Y., Fiorenza, E.A., Harvell, C.D., 2017. Seagrass ecosystems reduce exposure to bacterial pathogens of humans, fishes, and invertebrates. Science 355 (6326), 731. https://doi.org/10.1126/science.aal1956.
Lefcheck, J.S., Wilcox, D.J., Murphy, R.R., Marion, S.R., Orth, R.J., 2017. Multiple stressors threaten the imperiled coastal foundation species eelgrass (*Zostera marina*) in Chesapeake Bay, USA. Global Change Biol. 23, 3474–3483. https://doi.org/10.1111/gcb.13623.
Lefcheck, J.S., Hughes, B.B., Johnson, A.J., Pfirrmann, B.W., Rasher, D.B., Smyth, A.R., Orth, R.J., 2019. Are coastal habitats important nurseries? A meta-analysis. Conserv Lett 12, e12645. https://doi.org/10.1111/conl.12645.
Máñez-Crespo, J., Tuya, F., Fernández-Torquemada, Y., Royo, L., del Pilar-Ruso, Y., Espino, F., et al., 2020. Seagrass *Cymodocea nodosa* across biogeographical regions and times: differences in abundance, meadow structure and sexual reproduction. Mar. Environ. Res. 162, 105159. https://doi.org/10.1016/j.marenvres.2020.105159.
Morris, E.P., Peralta, G., Benavente, J., Freitas, R., Rodrigues, A.M., Quintino, V., Pérez-Lloréns, J.L., 2009. *Caulerpa prolifera* stable isotope ratios reveal anthropogenic nutrients within a tidal lagoon. Mar. Ecol. Prog. Ser. 390, 117–128. https://doi.org/10.3354/meps08184.
Muñoz, J.L., Sánchez de LaMadrid, A., 1994. El medio físico y biológico en la bahía de Cádiz: Saco interior. Junta de Andalucía. Consejería de Agricultura y Pesca.
Olesen, B., Krause-Jensen, D., Christensen, P.B., 2017. Depth-related changes in reproductive strategy of a cold-temperate *Zostera marina* meadow. Estuar. Coast 40, 553–563. https://doi.org/10.1007/s12237-016-0155-4.
Olivé, I., Vergara, J.J., Pérez-Lloréns, J.L., 2013. Photosynthetic and morphological photoacclimation of the seagrass *Cymodocea nodosa* to season, depth and leaf position. Mar. Biol. 160, 285–297. https://doi.org/10.1007/s00227-012-2087-2.
Ondiviela, B., Losada, I.J., Lara, J.L., Maza, M., Galván, C., Bouma, T.J., van Belzen, J., 2014. The role of seagrasses in coastal protection in a changing climate. Coast Eng. 87, 158–168, 0.1016/j.coastaleng.2013.11.005.
Orth, R.J., Carruthers, T.J.B., Dennison, W.C., Duarte, C.M., Fourqurean, J.W., Heck, K. L., et al., 2006. A global crisis for seagrass ecosystems. Bioscience 56, 987–996. https://doi.org/10.1641/0006-3568(2006)56[987:AGCFSE]2.0.CO;2.
Paar, M., Berthold, M., Schumann, R., Dahlke, S., Blindow, I., 2021. Seasonal variation in biomass and production of the macrophytobenthos in two lagoons in the southern baltic sea. Front. Earth Sci. 8, 542391. https://doi.org/10.3389/feart.2020.542391.
Pedersen, M.F., Borum, J., 1993. An annual nitrogen budget for a seagrass *Zostera marina* population. Mar. Ecol. Prog. Ser. 101, 169–177. https://doi.org/10.3354/meps101169.
Peduzzi, P., Vukovic, A., 1990. Primary production of *Cymodocea nodosa* in the Gulf of trieste (northern adriatic sea): a comparison of methods. Mar. Ecol. Prog. Ser. 64, 197–207. https://doi.org/10.3354/meps064197.
Peralta, G., Pérez-Lloréns, J.L., Hernández, I., Brun, F., Vergara, J.J., Bartual, A., García, C.M., 2000. Morphological and physiological differences between two morphotypes of *Zostera noltii* Hornem. From the south-western Iberian Peninsula. Helgol. Mar. Res. 54, 80–86. https://doi.org/10.1007/s101520050005.
Peralta, G., Pérez-Lloréns, J.L., Hernández, I., Vergara, J.J., 2002. Effects of light availability on growth, architecture and nutrient content of the seagrass *Zostera noltii* Hornem. J. Exp. Mar. Biol. Ecol. 269, 9–26. https://doi.org/10.1016/S0022-0981(01)00393-8.
Peralta, G., Brun, F.G., Hernández, I., Vergara, J.J., Pérez-Lloréns, J.L., 2005. Morphometric variations as acclimation mechanisms in *Zostera noltii* beds. Estuar. Coast Shelf Sci. 64, 347–356. https://doi.org/10.1016/j.ecss.2005.02.027.
Pérez-Hurtado, A., Goss-Custard, J.D., García, F., 1997. The diet of wintering waders in Cadiz Bay, southwest Spain. Hous. Theor. Soc. 44 (1), 45–52. https://doi.org/10.1080/00063659709461037.
Pérez-Lloréns, J.L., Niell, F.X., 1993. Seasonal dynamics of biomass and nutrient content in the intertidal seagrass *Zostera noltii* Hornem. From Palmones River estuary, Spain. Aquat. Bot. 46, 49–66. https://doi.org/10.1016/0304-3770(93)90064-4.
Pinheiro, J., Bates, D., DebRoy, S., Sarkar, D., R Core Team, 2019. Nlme: Linear and Nonlinear Mixed Effects Models. R Package Version 3.1-142. URL: https://CRAN.R-project.org/package=nlme.
R Core Team, 2019. R: A Language and Environment for Statistical Computing. R Foundation for Statistical Computing, Vienna, Austria. URL. https://www.R-project.org/.
Ricart, A.M., Ward, M., Hill, T.M., Sanford, E., Kroeker, K.J., Takeshita, Y., Gaylord, B., 2021. Coast-wide evidence of low pH amelioration by seagrass ecosystems. Global Change Biol. 27, 2580–2591. https://doi.org/10.1111/gcb.15594.
Roca, G., Alcoverro, T., Krause-Jensen, D., Balsby, T.J.S., Van Katwijk, M.M., Marbà, N., Romero, J., 2016. Response of seagrass indicators to shifts in environmental stressors: a global review and management synthesis. Ecol. Indicat. 63, 310–323. https://doi.org/10.1016/j.ecolind.2015.12.007.
Schubert, N., Colombo-Pallota, M.F., Enríquez, S., 2015. Leaf and canopy scale characterization of the photoprotective response to highlightstress of the seagrass *Thalassia testudinum*. Limnol. Oceanogr. 60, 286–302. https://doi.org/10.1002/lno.10024.
Sghaier, Y.R., Zakhama-Sraieb, R., Charfi-Cheikhrouha, F., 2017. Spatio-temporal dynamics and biomass of *Cymodocea nodosa* in bekalta (Tunisia, southern mediterranean sea). Mar. Ecol. 38, e12383 https://doi.org/10.1111/maec.12383.
Shaltout, M., Omstedt, A., 2014. Recent sea surface temperature trends and future scenarios for the Mediterranean Sea. Oceanologia 56, 411–443. https://doi.org/10.5697/oc.56-3.411.
Short, F.T., Carruthers, T.J.R., Waycott, M., Kendrick, G.A., Fourqurean, J.W., Callabine, Dennison, W.C., 2010. *Cymodocea Nodosa*. The IUCN Red List of Threatened Species 2010. https://doi.org/10.2305/IUCN.UK.2010-3.RLTS.T153535A4516419.en. T153535A4516419.
Sievers, M., Brown, C.J., Tulloch, V.J., Pearson, R.M., Haig, J.A., Turschwell, M.P., Connolly, R.M., 2019. The role of vegetated coastal wetlands for marine megafauna conservation. Trends Ecol. Evol. 34, 807–817. https://doi.org/10.1016/j.tree.2019.04.004.
Suykerbuyk, W., Govers, L.L., van Oven, W.G., Giesen, K., Giesen, W.B.J.T., Jong, D.J., van Katwijk, M.M., 2018. Living in the intertidal: desiccation and shading reduce seagrass growth, but high salinity or population of origin have no additional effect. PeerJ 6, e5234. https://doi.org/10.7717/peerj.5234.

Tanaka, Y., Nakaoka, M., 2004. Emergence stress and morphological constraints affect the species distribution and growth of subtropical intertidal seagrasses. Mar. Ecol. Prog. Ser. 284, 117–131. https://doi.org/10.3354/meps284117.

Terrados-Muñoz, J., 1995. Effects of some plant growth regulators on the growth of the seagrass *Cymodocea nodosa* (Ucria) Ascherson. Aquat. Bot. 51, 311–318. https://doi.org/10.1016/0304-3770(95)00481-E.

UNEP, 2020. Out of the Blue: the Value of Seagrasses to the Environment and to People. UNEP, Nairobi.

Unsworth, R.K.F., DeLeon, P.S., Garrard, S.L., Jompa, J., Smith, D.J., Bell, J.J., 2008. High connectivity of Indo-Pacific seagrass fish assemblages with mangrove and coral reef habitats. Mar. Ecol. Prog. Ser. 353, 213–224. https://doi.org/10.3354/meps07199.

Unsworth, R.K., Nordlund, L.M., Cullen-Unsworth, L.C., 2019. Seagrass meadows support global fisheries production. Conserv Lett 12, e12566. https://doi.org/10.1111/conl.12566.

Waycott, M., Collier, C., McMahon, K., Ralph, P., McKenzie, L., Udy, J., Grech, A., 2007. Vulnerability of seagrasses in the great barrier reef to climate change. In: Johnson, J. E., Marshall, P.A. (Eds.), Climate Change and the Great Barrier Reef. Great Barrier Reef Marine Park Authority and Australian Greenhouse Office, pp. 193–236.

Westoby, M., Howell, J., 1986. Influence of population structure on self-thinning of plant populations. J. Ecol. 74, 343–359. https://doi.org/10.2307/2260259.

Winslow, L.A., Zwart, J.A., Batt, R.D., Dugan, H.A., Woolway, R.I., Corman, J.R., Read, J. S., 2016. LakeMetabolizer: an R package for estimating lake metabolism from free-water oxygen using diverse statistical models. Inland Waters 6 (4), 622–636. https://doi.org/10.1080/IW-6.4.883.

Zuur, A., Ieno, E.N., Walker, N., Saveliev, A.A., Smith, G.M., 2009. Mixed Effects Models and Extensions in Ecology with R, 2009th ed. Springer, ISBN 978-0-387-87457-9. https://doi.org/10.1007/978-0-387-87458-6.